Protein Science (1998), 7:2669–2674. Cambridge University Press. Printed in the USA.

FOR THE RECORD

Solution structure of the His12 → Cys mutant of the N-terminal zinc binding domain of HIV-1 integrase complexed to cadmium

MENGLI CAI,[1] YING HUANG,[2] MICHAEL CAFFREY,[1] RONGLAN ZHENG,[2] ROBERT CRAIGIE,[2] G. MARIUS CLORE,[1] AND ANGELA M. GRONENBORN[1]

[1]Laboratory of Chemical Physics, Building 5, National Institute of Diabetes and Digestive and Kidney Diseases, National Institutes of Health, Bethesda, Maryland 20892-0520
[2]Laboratory of Molecular Biology, Building 5, National Institute of Diabetes and Digestive and Kidney Diseases, National Institutes of Health, Bethesda, Maryland 20892-0520

(RECEIVED June 18, 1998; ACCEPTED August 18, 1998)

Abstract: The solution structure of His12 → Cys mutant of the N-terminal zinc binding domain (residues 1–55; IN^{1-55}) of HIV-1 integrase complexed to cadmium has been solved by multidimensional heteronuclear NMR spectroscopy. The overall structure is very similar to that of the wild-type N-terminal domain complexed to zinc. In contrast to the wild-type domain, however, which exists in two interconverting conformational states arising from different modes of coordination of the two histidine side chains to the metal, the cadmium complex of the His12 → Cys mutant exists in only a single form at low pH. The conformation of the polypeptide chain encompassing residues 10–18 is intermediate between the two forms of the wild-type complex.

Keywords: cadmium; conformational states; HIV-1; integrase; N-terminal domain

HIV integrase comprises three functional and structural domains whose structures have been solved: a central catalytic core (Dyda et al., 1994), an N-terminal zinc binding domain (Cai et al., 1997; Eijkelenboom et al., 1997) and a C-terminal DNA binding domain (Eijkelenboom et al., 1995; Lodi et al., 1995). The catalytic core is capable of catalyzing a phosphoryl transfer reaction termed disintegration, but requires the presence of the two other domains for 3′ processing and DNA strand transfer (Bushman et al., 1993). The N-terminal domain of HIV-1 integrase (IN^{1-55}) is unstructured in the absence of zinc, but in the presence of zinc folds into a well-defined dimeric structure comprising four helices per subunit (Cai et al., 1997). The zinc is coordinated by His12, His16, Cys40, and Cys43. Interestingly, the IN^{1-55}-Zn^{2+} complex exists in two interconverting conformational states, termed E and D, differing in the nature of the metal coordination by the two histidine residues (Cai et al., 1997). In both forms, His16 coordinates the zinc via its Nδ1 atom. In the E form, which predominates below 300 K at pH 7.4, His12 is buried within the protein interior, coordinates the zinc via its Nε2 atom and donates a hydrogen bond through its Nδ1H proton to the sulfur of Met22, while His16 is solvent exposed. In the D form, the relative positions of His12 and His16 are reversed, such that His12 is solvent exposed and like His16 coordinates the zinc via its Nδ1 atom. The different histidine arrangements are associated with large conformational differences in the polypeptide backbone (residues 9–18) around the coordinating histidines. The dimer interface, which is identical in the two forms, is predominantly hydrophobic and is formed by the packing of the N-terminal end of helix 1, helix 3, and helix 4. To alleviate problems arising from the presence of the two interconverting forms we have pursued avenues that would result in the predominance of one molecular species. In this paper, we report on a mutant in which His12 is replaced by a cysteine and present the three-dimensional structure of the cadmium complex of this variant.

The rationale for our strategy was based on the knowledge that Cd^{2+} binding to His_2Cys_2 metal clusters is generally of lower affinity than Zn^{2+} binding (Alexander et al., 1993; Krizek et al., 1993), but that a dramatic increase in Cd^{2+} affinity is observed as the number of thiolate ligands is increased (Krizek et al., 1993). In complete agreement with these prior observations, we observed multiple forms for IN^{1-55}(H12C) when complexed with Zn^{2+}, whereas the Cd^{2+} substituted protein existed in a single conformation at pH 4.5, as judged by the ^1H-^{15}N correlation spectrum which exhibited only a single set of resonances per residue (Fig. 1). A long range ^1H-^{15}N correlation spectrum in which the nitrogen and carbon-attached proton resonances of the histidine side chain are correlated showed that the Nδ1 and Nε2 atoms of His16 resonated in the 170–173 ppm range (Pelton et al., 1993),

Reprint requests to: G.M. Clore or A.M. Gronenborn, Laboratory of Chemical Physics, Building 5, National Institute of Diabetes and Digestive and Kidney Diseases, National Institutes of Health, Bethesda, Maryland 20892-0520; e-mail: clore@speck.niddk.nih.gov or gronenborn@vger.niddk.nih.gov.

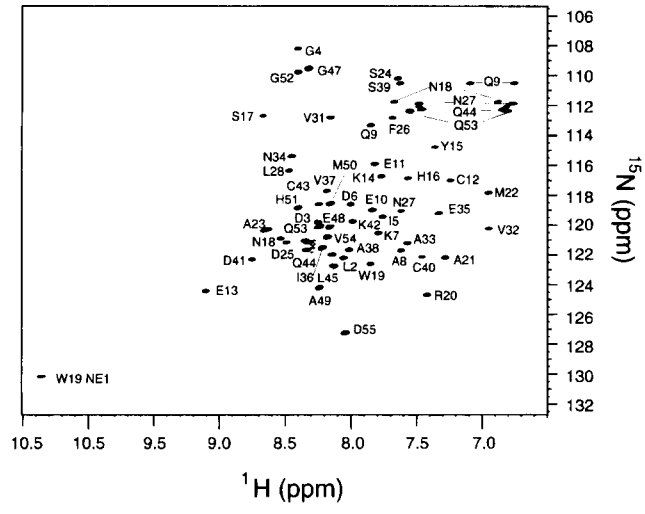

Fig. 1. ^{1}H-^{15}N HSQC spectrum of the IN$^{1-55}$(H12C)-Cd^{2+} complex.

indicating that His16 is protonated at pH 4.5. Hence, His16 cannot be coordinated to cadmium. At higher pH values, additional forms of the Cd^{2+} complex are observed, most likely due to coordination by the imidazole ring of His16. Figure 2 provides a qualitative comparison of the structural and dynamics properties of IN$^{1-55}$(H12C)-Cd^{2+} complex and the E and D forms of the wild-type IN$^{1-55}$-Zn^{2+} complex in terms of the secondary $^{13}C\alpha$ shifts and heteronuclear ^{15}N-{^{1}H} nuclear Overhause effect (NOE) values. While the position and length of helices 2 and 3 (residues 19–25 and 30–39) are the same in the three complexes, clear differences are observed in the length of helix 1 and the structure of the loop connecting helices 1 and 2. In the Cd^{2+} complex helix 1 extends from residues 3 to 10 and there is a small helical turn from residues 12 to 14. In the E form of the IN$^{1-55}$-Zn complex helix 1 extends from residues 2–14, and in the D form from residues 2 to 8 followed by a helical turn from residues 14–17. In addition, the ^{15}N-{^{1}H} NOEs indicate that helix 4 is more mobile in the IN$^{1-55}$(H12C)-Cd^{2+} complex than in either the E or D forms of the wild-type complex. This accounts for the small secondary $^{13}C\alpha$ shifts observed for helix 4 (residues 41–45) in the IN$^{1-55}$(H12C)-Cd^{2+}. The average conformation of helix 4, however, is defined by nonsequential NOEs between residues 37 and 43, 40 and 42, 40 and 43, 41 and 44, and 42 and 45.

The structure of the IN$^{1-55}$(H12C)-Cd^{2+} complex was solved by multidimensional heteronuclear NMR (Clore & Gronenborn, 1991, 1998a; Bax & Grzesiek, 1993) on the basis of 640 experimental NMR restraints per monomer (including 20 intermolecular NOEs identified in a three-dimensional ^{13}C-edited/^{12}C-filtered NOE spectrum). A summary of the structural statistics is provided in Table 1, and a best fit superposition of the 40 simulated annealing structures of the IN$^{1-55}$(H12C)-Cd^{2+} complex is shown in Figure 3. The ordered portion of the structure comprising residues 1–45 is well defined with a backbone precision for the dimer of 0.4 Å and ~93% of the residues lying in the most favourable region of the Ramachandran ϕ,ψ map. The orientation of the two subunits in the dimer is identical to that of the wild-type IN$^{1-55}$-Zn^{2+} complex. The RMS difference between the mean coordinates of the Cd^{2+} complex and the E and D forms of the Zn^{2+} complex is 1.1 Å (excluding residues 15–17) and 0.9 Å (excluding residues 11–14), respectively.

A ribbon diagram comparing the monomer structure of the three complexes is shown in Fig. 4. The position of the coordinating metal ion and the conformation of Cys40 and Cys43 is the same in all three complexes. Cys12 in the IN$^{1-55}$(H12C)-Cd^{2+} complex

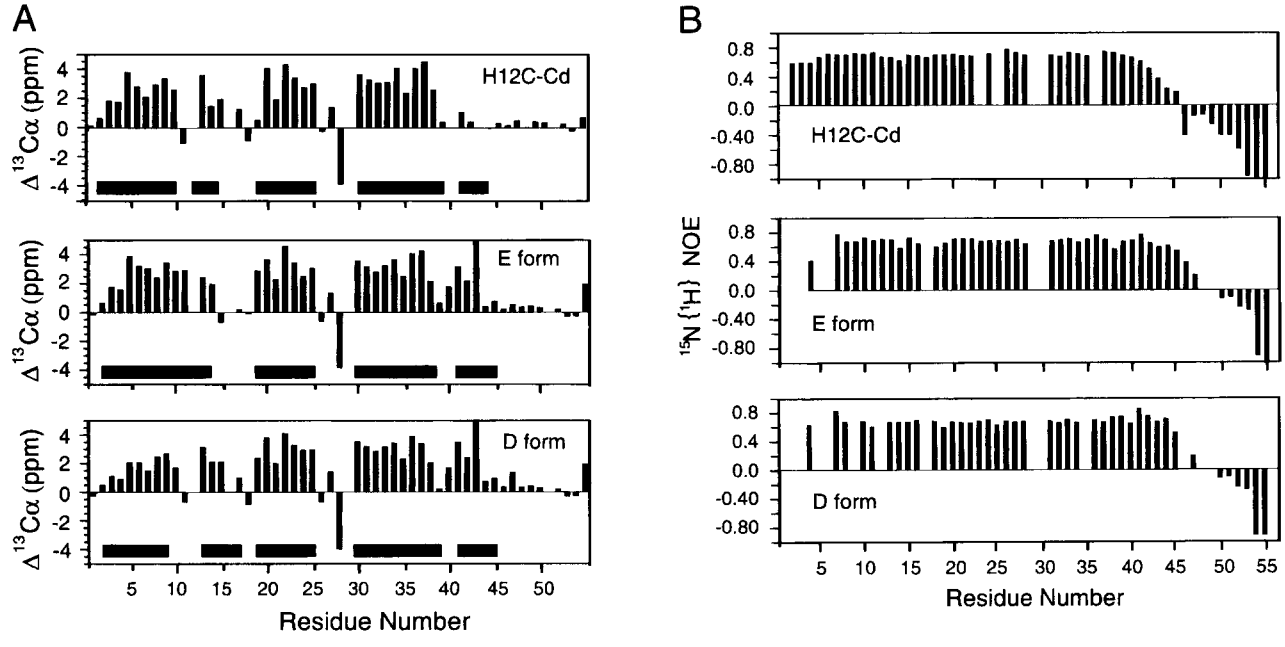

Fig. 2. (**A**) Secondary $^{13}C\alpha$ shifts and (**B**) ^{15}N-{^{1}H} NOEs for the IN$^{1-55}$(H12C)-Cd^{2+} complex and the E and D forms of the wild-type IN$^{1-55}$-Zn^{2+} complex. The solid horizontal bars in **A** indicate the location of the helical segments.

Table 1. *Structural statistic*[a]

	$\langle SA \rangle$	$\langle \overline{SA} \rangle r$
Structural statistics		
RMS deviations from experimental distance restraints (Å)[b]		
All (494)	0.031 ± 0.003	0.035
Intrasubunit		
Interresidue sequential ($\|i - j\| = 1$) (203)	0.025 ± 0.008	0.022
Interresidue short range ($1 < \|i - j\| \leq 5$) (161)	0.038 ± 0.002	0.043
Interresidue long range ($\|i - j\|) > 5$) (82)	0.024 ± 0.005	0.024
Intraresidue (5)[c]	0.000 ± 0.000	0.000
H-bonds (16)	0.003 ± 0.005	0.000
Intersubunit (20)[d]	0.053 ± 0.013	0.094
Ambiguous intra- and intersubunit (7)[e]	0.003 ± 0.005	0.000
RMS deviations from experiment		
Dihedral restraints (deg) (117)[b]	0.184 ± 0.071	0.340
RMS deviations from experiment		
$^3J_{HN\alpha}$ coupling constants (Hz) (47)[b]	0.65 ± 0.02	0.74
RMS deviations from experimental ^{13}C shifts		
$^{13}C\alpha$ (ppm) (50)	1.14 ± 0.04	1.16
$^{13}C\beta$ (ppm) (49)	0.81 ± 0.05	0.82
Deviations from idealized covalent geometry		
Bonds (Å) (848)	0.003 ± 0.0004	0.005
Angles (deg) (1,536)	0.553 ± 0.109	0.587
Impropers (deg) (439)	0.341 ± 0.031	0.411
Measures of structure quality		
E_{L-J}[f] (kcal mol^{-1})	−435 ± 12	−385
PROCHECK[g]		
% residues in most favorable region of Ramachandran plot	93.4 ± 1.4	92.5
Number of bad contacts/100 residues	5.4 ± 1.6	4.4
Coordinate precision of the dimer[h]		
Backbone (Å)	0.40 ± 0.08	
All atoms (Å)	0.72 ± 0.07	

[a]The notation of the NMR structures is as follows: $\langle SA \rangle$ are the final 40 simulated annealing structures; $\overline{SA}$ is the mean structure obtained by averaging the coordinates of the individual *SA* structures (residues 1–45 of both subunits) best fitted to each other; $\langle \overline{SA} \rangle r$ is the restrained minimized mean structure obtained by restrained regularization of the mean structure $\overline{SA}$. The number of terms for the various restraints per monomer is given in parentheses. The final force constants employed for the various terms in the target function used for simulated annealing are as follows: 1,000 kcal mol^{-1} Å^{-2} for bond lengths, 500 kcal mol^{-1} rad^{-2} for angles and improper torsions (which serve to maintain planarity and chirality), 30 kcal mol^{-1} Å^{-2} for the S-Cd^{2+} bond length, 10 kcal mol^{-1} rad^{-2} for the S-Cd^{2+}-S bond angle, 100 kcal mol^{-1} Å^{-2} for noncrystallographic symmetry, 4 kcal mol^{-1} Å^{-4} for the quartic van der Waals repulsion term (with the hard sphere effective van der Waals radii set to 0.8 times their value used in the CHARMM PARAM19/20 parameters), 30 kcal mol^{-1} Å^{-2} for the experimental distance restraints (interproton distances and hydrogen bonds), 200 kcal mol^{-1} rad^{-2} for the torsion angle restraints, 1 kcal mol^{-1} Hz^{-2} for the coupling constant restraints, 0.5 kcal mol^{-1} ppm^{-2} for the carbon chemical shift restraints, and 1.0 for the conformational database potential. The latter is based on the populations of various combinations of torsion angles observed in a database of 70 high-resolution (1.75 Å or better) X-ray structures and biases sampling to conformations that are energetically possible by effectively limiting the choice of dihedral angles to those that are known to be physically realizable (Clore & Gronenborn, 1998b).

[b]None of the structures exhibited distance violations greater than 0.5 Å, dihedral angle violations greater than 5°, or $^3J_{HN\alpha}$ coupling constant violations greater than 2 Hz. The torsion angles restraints comprise 45ϕ, 35ψ, $26\chi_1$, $10\chi_2$, and $1\chi_3$ angle per monomer.

[c]Only structurally useful intraresidue NOEs are included in the intraresidue interproton distance restraints. Thus, intraresidue NOEs between protons separated by two bonds or between nonstereospecifically assigned protons separated by three bonds are not incorporated in the restraints.

[d]Intersubunit NOEs from protons attached to ^{13}C (in the indirect dimension) to protons attached to ^{12}C (in the acquisition dimension) were obtained from a three-dimensional ^{13}C-separated/^{12}C-filtered NOE spectrum recorded on a sample containing a 1:1 mixture of $^{15}N/^{13}C$ and $^{14}N/^{12}C$ (natural isotopic abundance) labeled IN$^{1-55}$(H12C)-Cd^{2+} complex.

[e]NOEs where a distinction between intra- and intersubunit effects could not be distinguished were treated as $(\Sigma r^{-6})^{-1/6}$ sums (Nilges, 1993).

[f]E_{L-J} is the Lennard–Jones van der Waals energy calculated with the CHARMM PARAM19/20 protein parameters (Brooks et al., 1993) and is not included in the target function for simulated annealing or restrained minimization.

[g]The program PROCHECK (Laskowski et al., 1993) was used to assess the overall quality of the structures. The dihedral angle *G*-factors for the ϕ/ψ, χ_1/χ_2, χ_1, and χ_3/χ_4 distributions are 0.48 ± 0.04, 0.78 ± 0.08, 0.34 ± 0.13, and 0.32 ± 0.18, respectively. The PROCHECK statistics apply to the ordered region of IN$^{1-55}$(H12C) comprising residues 1–45 of the two subunits.

[h]The precision of the atomic coordinates is defined as the average RMS difference between the 40 final simulated annealing structures and the mean coordinates, $\overline{SA}$. The values given relate to residues 1–45 of the two subunits together. The backbone atoms comprise the N, Cα, C, and O atoms.

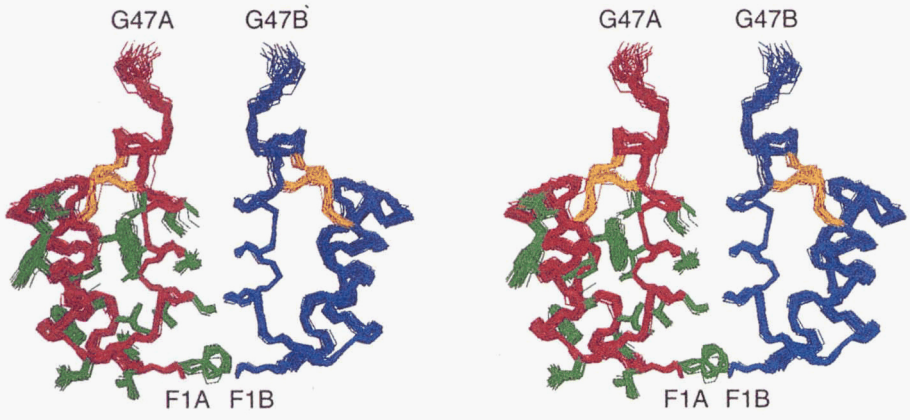

Fig. 3. Stereoviews showing superpositions of the backbone atoms, cadmium, and coordinating cysteines of the $IN^{1-55}(H12C)$-Cd^{2+} dimer. Residues 1–47 of each subunit are displayed; the backbone of one monomer is shown in red and of the other in blue; the cadmium and coordinating Cys residues are shown in yellow; and ordered side chains on one monomer only are displayed in green. The C-terminal region extending from residues 48–55 is not shown since it is disordered as judged by the ^{15}N-$\{^1H\}$ NOE data shown in Figure 2B and the absence of any nonsequential interresidue ^1H-^1H NOEs.

occupies the same position as His12 in the E form of the wild-type zinc complex. His16, however, is protonated and no longer coordinated to the metal in $IN^{1-55}(H12C)$-Cd^{2+} complex. The fourth coordinating position of the cadmium is presumably occupied by water. Indeed, the ^{113}Cd chemical shift of 538 ppm observed for the complex is consistent with a S_3O coordination (Colman, 1993). It is also noted that, while Tyr15 is in the same side-chain rotamer for all three complexes, its position with respect to helix 2 differs as a result of the large changes in backbone conformation involving residues 10–18 associated with the different types of metal coordination observed.

In proteins, structural metal binding sites provide a unique way of increasing the range of conformations (and activities) during evolution, exploiting the large free energy of metal binding to stabilize the optimal protein structure. In this study, we have shown that it is possible to stabilize a single conformation of the IN^{1-55} domain of HIV-1 integrase by mutating one of the coordinating histidine residues in the wild-type sequence (His12) to a cysteine, resulting in preferential cadmium coordination over zinc.

Experimental: *Expression and purification:* Protein expression and purification of $IN^{1-55}(H12C)$ were as described previously (Cai et al., 1998), and samples were prepared at natural isotopic abundance, with uniform ^{15}N (>95%) labeling, and with uniform ^{15}N and ^{13}C (>95%) labeling. The reverse phase HPLC purified protein was first dialyzed in 50 mM NH_4HCO_3, 10 mM EDTA, and 10 mM DTT, followed by dialysis in deionized water containing 20 mM β-mercaptoethanol, with the external buffer changed three times. The dialyzed protein solution was then lyophilized with 100 mM β-mercaptoethanol, and subsequently dissolved in buffer containing 25 mM Tris pH 7.4, 200 mM NaCl, and 5 mM cadmium acetate. The pH of the protein solution was then adjusted to pH 4.5 with either 5% acetic acid or 1 M NaOH. The following samples were prepared: ^{15}N-labeled $IN^{1-55}(H12C)$-Cd^{2+} in 95% H_2O/5% D_2O; $^{15}N/^{13}C$-labeled $IN^{1-55}(H12C)$-Cd^{2+} in 95% H_2O/5% D_2O and 99.996% D_2O; heterodimer containing a 1:1 mixture of $^{15}N/^{13}C$ and $^{14}N/^{12}C$-labeled $IN^{1-55}(H12C)$-Cd^{2+} in 99.996% D_2O. In addition, a sample containing $^{113}Cd^{2+}$ was prepared.

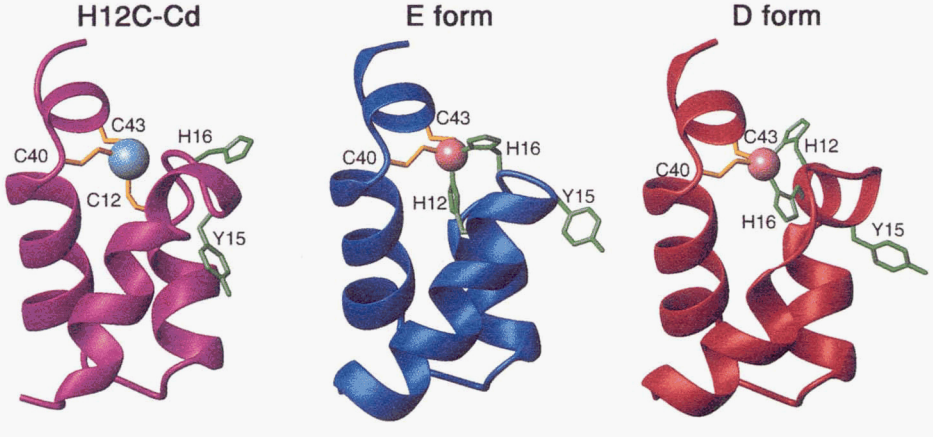

Fig. 4. Ribbon diagrams illustrating the monomer of the $IN^{1-55}(H12C)$-Cd^{2+} complex (left) and the E (middle) and D (right) forms of the wild-type IN^{1-55}-Zn^{2+} complex. Cadmium and zinc are displayed as light blue and pink balls, respectively.

NMR spectroscopy: Multidimensional NMR experiments were carried out at 30 °C on Bruker DMX500 and DMX600 spectrometers equipped with x,y,z-shielded gradient triple resonance probes. Spectra were processed with the NMRPipe package (Delaglio et al., 1995), and analyzed using the programs PIPP, CAPP, and STAPP (Garrett et al., 1991). A one-dimensional ^{113}Cd spectrum of the IN$^{1-55}$(H12C)-Cd^{2+} was recorded on a Bruker DMX 500 spectrometer, and the ^{113}Cd chemical shift in the complex is reported relative to 0.1 M $Cd(ClO_4)_2$ (Colman, 1993). The sequential assignment of the ^{1}H, ^{13}C, and ^{15}N chemical shifts was achieved by means of through-bond heteronuclear correlations along the backbone and side chains (Clore & Gronenborn, 1991, 1998a; Bax & Grzesiek, 1993). $^3J_{HN\alpha}$, $^3J_{NH\beta}$, $^3J_{C'C\gamma}$(aromatic, methyl, and methylene), $^3J_{NC\gamma}$(aromatic, methyl, and methylene) couplings were obtained by quantitative J correlation spectroscopy (Bax et al., 1994). Interproton distance restraints were derived from the following spectra: three-dimensional ^{15}N-separated (120 ms mixing time), three-dimensional ^{13}C-separated (50 and 120 ms mixing times), and three-dimensional ^{13}C-separated/^{12}C-filtered (150 ms mixing time) NOE spectra, three-dimensional ^{15}N-separated ROE (40 ms mixing time) spectrum, and four-dimensional ^{13}C/^{15}N-separated (120 and 150 ms mixing times) and four-dimensional ^{13}C/^{13}C-separated (150 ms mixing time) NOE spectra. ^{15}N{^{1}H} NOE values were measured as described by Grzesiek and Bax (1993). Long-range nitrogen-proton correlations involving the histidine rings were observed in a ^{1}H-^{15}N HSQC spectrum recorded with a 22 ms dephasing delay during which time the ^{1}H and ^{15}N signals become antiphase (Pelton et al., 1993).

Structure calculations: Approximate interproton distance restraints were derived from the multidimensional NOE spectra, essentially as described previously (Clore & Gronenborn, 1991). NOEs were grouped into four distance ranges, 1.8–2.7 Å (1.8–2.9 Å for NOEs involving NH protons), 1.8–3.3 Å (1.8–3.5 Å for NOEs involving NH protons), 1.8–5.0 and 1.8–6.0 Å, corresponding to strong, medium, weak, and very weak NOEs. 0.5 Å was added to the upper bounds for distances involving methyl groups to account for the higher apparent intensity of the methyl resonances. Distances involving methyl groups, aromatic ring protons, nonstereospecifically assigned methylene protons, and groups where a distinction between intermolecular and intramolecular effects could not be distinguished were represented as a $(\Sigma r^{-6})^{-1/6}$ sum (Nilges, 1993). Protein backbone hydrogen bonding restraints (two per hydrogen bond, $r_{NH\text{-}O}$ = 1.5–2.8 Å, $r_{N\text{-}O}$ = 2.4–3.5 Å) within areas of regular secondary structure were introduced during the final stages of refinement using standard NMR criteria based on backbone NOEs and $^3J_{HN\alpha}$ coupling constants, supplemented by secondary $^{13}C\alpha/\beta$ shifts. ϕ, ψ, χ_1, and χ_2 torsion angle restraints were derived from the NOE/ROE and homo- and heteronuclear three-bond coupling constant data, and the minimum ranges employed were ±15°, ±40°, ±20°, and ±30°, respectively (Cai et al., 1997). The structures were calculated by simulated annealing (Nilges et al., 1988) using the program CNS (Brünger et al., 1998) adapted to incorporate pseudo-potentials for $^3J_{HN\alpha}$ coupling constant and secondary $^{13}C\alpha/^{13}C\beta$ chemical shift restraints, and a conformational database potential (Clore & Gronenborn, 1998b). The target function that is minimized during simulated annealing and restrained regularization comprises quadratic harmonic potential terms for covalent geometry, noncrystallographic symmetry, and $^3J_{HN\alpha}$ coupling constant and secondary $^{13}C\alpha$ and $^{13}C\beta$ chemical shift restraints, square-well quadratic potentials for the experimental distance and torsion angle restraints, a quartic van der Waals repulsion term for the nonbonded contacts, and a conformational database potential. The S-Cd bond lengths and the S-Cd-S bond angles were restrained to 2.6 Å and 109°, respectively, using force constants of 30 kcal mol^{-1} Å^{-2} and 10 kcal mol^{-1} rad^{-2}, respectively. There were no hydrogen-bonding, electrostatic, or 6–12 Lennard–Jones empirical potential energy terms in the target function. Figures were generated using the programs MOLMOL (Koradi et al., 1996).

The coordinates of the final 40 simulated annealing structures and of the restrained regularized mean structure, and the complete list of experimental NMR restraints and ^{1}H, ^{15}N, ^{13}C chemical shift assignments (accession codes 1WJF, 1WJE, and R1WJEMR) have been deposited in the Brookhaven Protein Data Bank.

Acknowledgments: We thank Dan Garrett and Frank Delaglio for software support, Rolf Tschudin for technical support, and Marcel Ottiger and Nico Tjandra for useful discussions. This work was supported by the AIDS Targeted Antiviral Program of the Office of the Director of the National Institutes of Health (to G.M.C., A.M.G., and R.C.).

References

Alexander RS, Kiefer LL, Fierka CA, Christianson DW. 1993. Engineering the zinc-binding site of human carbonic anhydrase II: Structure of the His94 → Cys apoenzyme in a new crystalline form. *Biochemistry 32*:1510–1518.

Bax A, Grzesiek S. 1993. Methodological advances in protein NMR. *Acct Chem Res 26*:131–138.

Bax A, Vuister GW, Grzesiek S, Delaglio F, Wang AC, Tschudin R, Zhu G. 1994. Measurement of homo- and heteronuclear J couplings from quantitative J correlation. *Meth Enzymol 239*:79–106.

Brooks BR, Bruccoleri RE, Olafson BD, States DJ, Swaminathan S, Karplus M. 1993. CHARMM: A program for macromolecular energy minimization and dynamics calculations. *J Comput Chem 4*:187–217.

Brünger AT, Adams PD, Clore GM, DeLano WL, Gros P, Grosse-Kunstleve RW, Jiang JS, Kuszewski J, Nilges M, Pannu NS, Read RJ, Rice LM, Simonson T, Warren GL. 1998. Crystallography and NMR system (CNS): A new software suite for macromolecular structure determination. *Acta Cryst D54*: 905–921.

Bushman FD, Engelman A, Palmer I, Wingfield PT, Craigie R. 1993. Domains of integrase protein of human immunodeficiency virus type-1 responsible for polynucleotidyl transfer and zinc binding. *Proc Natl Acad Sci USA 90*:3428–3432.

Cai M, Huang Y, Sakaguchi K, Clore GM, Gronenborn AM, Craigie R. 1998. An efficient and cost-effective isotope labeling protocol for proteins expressed in *Escherichia coli*. *J Biomol NMR 11*:97–102.

Cai M, Zheng R, Caffrey M, Craigie R, Clore GM, Gronenborn AM. 1997. Solution structure of the N-terminal zinc binding domain of HIV-1 integrase. *Nature Struct Biol 4*:567–577.

Clore GM, Gronenborn AM. 1998a. Determining the structure of large proteins and protein complexes by NMR. *Trends Biotech 16*:22–34.

Clore GM, Gronenborn AM. 1998b. New methods of structure refinement for macromolecular structure determination by NMR. *Proc Natl Acad Sci USA. 95*:5891–5898.

Clore GM, Gronenborn AM. 1991. Structures of larger proteins in solution: Three- and four-dimensional heteronuclear NMR spectroscopy. *Science 252*:1390–1399.

Colman JE. 1993. Cadmium-113 nuclear magnetic resonance applied to metalloproteins. *Methods Enzymol 227*:16–43.

Delaglio F, Grzesiek S, Vuister GW, Zhu G, Pfeifer J, Bax A. 1995. NMRPipe: A multidimensional spectral processing system based on UNIX pipes. *J Biomolec NMR 6*:277–293.

Dyda F, Hickman AB, Jenkins TM, Engelman A, Craigie R, Davies DR. 1994. Crystal structure of the catalytic domain of HIV-1 integrase: Similarity to other polynucleotidyl transferases. *Science 266*:1981–1986.

Garrett DS, Powers R, Gronenborn AM, Clore GM. 1991. A common sense approach to peak picking in two-, three- and four-dimensional spectra using automatic computer analysis of contour diagrams. *J Magn Reson 95*:214–220.

Grzesiek S, Bax A. 1993. The importance of not saturating H_2O in protein

NMR: Application to sensitivity enhancement and NOE measurements. *J Am Chem Soc 115*:12593–12594.

Eijkelenboom AP, Lutzke RA, Boelens R, Plasterk RHA, Kaptein R, Hard K. 1995. The DNA binding domain of HIV-1 integrase has an SH3-like fold. *Nature Struct Biol 2*:807–810.

Eijkelenboom APAM, van den Ent FMI, Vos A, Doreleijers JF, Hard K, Tuluis TD, Pasterk RHA, Kaptein R, Boelens R. 1997. The solution structure of the amino-terminal HHCC domain of HIV-2 integrase: A three-helix bundle stabilized by zinc. *Curr Biol 7*:739–746.

Koradi R, Billeter M, Wüthrich K. 1996. MOLMOL: A program for display and analysis of macromolecular structures. *J Mol Graphics 14*:52–55.

Krizek BA, Merkle DL, Berg JM. 1993. Ligand variation and metal ion specificity in zinc finger proteins. *Inorg Chem 32*:937–940.

Laskowski RA, MacArthur MW, Moss DS, Thornton JM. 1993. PROCHECK: A program to check stereochemical quality of protein structures. *J Appl Crystallogr 26*:283–291.

Lodi PJ, Ernst JA, Kuszewski J, Hickman AB, Engelman A, Craigie R, Clore GM, Gronenborn AM. 1995. Solution structure of the DNA binding domain of HIV-1 integrase. *Biochemistry 34*:9826–9833.

Nilges M. 1993. A calculational strategy for the structure determination of symmetric dimers by ^{1}H NMR. *Proteins Struct Funct Genet 17*:297–309.

Nilges M, Clore GM, Gronenborn AM. 1988. Determination of three-dimensional structures of proteins from interproton distance data by hybrid distance geometry-dynamical simulated annealing calculations. *FEBS Lett 229*:317–324.

Pelton JG, Torchia DA, Meadow MD, Roseman S. 1993. Tautomeric states of the active-site histidines of phosphorylated and unphosphorylated III^{Glc}, a signal transducing protein from *Escherichia coli*, using two-dimensional heteronuclear NMR techniques. *Protein Sci 2*:543–558.